Suplemento de la Revista Mexicana de Física **3** 0308088 (2022) 1–5

Charm production and hadronisation in ALICE

Benedikt Volkel on behalf of the ALICE collaboration
CERN, Espl. des Particules 1, 1211 Meyrin, Geneva, Switzerland.

Received 30 December 2021; accepted 25 February 2022

Heavy-flavour production is an active and highly interesting field of research. Since charm and beauty quarks are predominantly produced in the hard scattering process of colliding nuclei, they serve as unique probes to study the quark-gluon plasma in Pb–Pb collisions. In addition, recent investigations of hadronisation mechanisms have revealed interesting and unexpected features when comparing measurements in e^+e^- and in hadronic collisions as in pp, p–Pb and Pb–Pb. This article summarises the latest results of charm production measured by the ALICE Collaboration. For the first time, $\Sigma_c^{0,++}$ and Ω_c^0 were measured in hadronic collisions and production measurements of the Λ_c^+ and Ξ_c^0 are now included in the computation of the charm production cross section.

Keywords: Charm production; hadronisation; heavy ion physics; high energy physics; ALICE.

DOI: https://doi.org/10.31349/SuplRevMexFis.3.0308088

1. Introduction

The study of hadron formation is an active field of research. Hadronisation cannot be described analytically in the framework of quantum chromodynamics (QCD) as perturbative approaches break down at the corresponding energy scales. For instance, phenomenological models based on string fragmentation [1] are commonly used to describe hadronisation in proton–proton (pp) collisions. By means of the factorisation approach [2], cross section calculations can be disentangled into different components separating terms describing the long-distance (low-energy) from the short-distance (high-energy) particle interaction. In particular, perturbative calculations based on the general-mass variable-flavour-number-scheme (GM-VFNS) [3, 4] as well as those based on fixed order with next-to-leading-logarithm resummation (FONLL) [5, 6] have shown good agreement in the case of strange and non-strange charm mesons. On the other hand, models based on collinear factorisation and fragmentation functions tuned to measurements in ^{e} and e^-p collisions provide only a poor description of charm baryon production, for instance as measured in the case of Λ_c^+ production [7–10].

Production measurements of different hadron species as well as their yield ratios provide powerful observables to experimentally constrain phenomenological hadronisation models. In this article, an overview of most recent charm baryon production measurements, namely Λ_c^+, $\Sigma_c^{0,++}$, $\Xi_c^{0,+}$, and Ω_c^0, conducted with the ALICE detector [11] is reported. It is worth noting that $\Sigma_c^{0,++}$ and Ω_c^0 productions were measured for the first time in hadronic collisions. Comparisons to various models are discussed and the charm fragmentation fractions measured for the first time in pp collisions by the ALICE Collaboration are presented as well. The total charm production cross section has been measured in pp collisions at $\sqrt{s} = 5.02\,\mathrm{TeV}$ in the rapidity region of $|y| < 0.5$ also accounting for the charm baryons Λ_c^+ and Ξ_c^0. Its current value is measured to be $(\mathrm{d}\sigma^{c\bar{c}}/\mathrm{d}y)\big|_{|y|<0.5} = 1165 \pm 44(\text{stat})^{+134}_{-101}(\text{syst})\,\mu\mathrm{b}$ [8].

2. Experimental setup and data samples

A detailed description of the ALICE detector can be found in [11]. It provides excellent tracking and particle identification (PID) capabilities, especially towards low transverse momentum (p_T). The principal sub-detectors involved in the following presented analyses were the Inner Tracking System (ITS) used for vertex finding and tracking, the Time Projection Chamber (TPC) for tracking and PID, the Time-Of-Flight detector (TOF) for PID, as well as the V0 detector for triggering purposes and event multiplicity estimation.

Tracks were reconstructed in the barrel region within the pseudorapidity window of $|\eta| < 0.8$. Depending on the decay channel of the various baryons under study, they were reconstructed from the combination of 2 or 3 tracks that passed the selection criteria. Background was suppressed by requiring the appropriate decay topologies of interest and by requiring suitable PID criteria. For details the reader is referred to the individual cited papers.

Results presented here were obtained in different collision systems and at two centre-of-mass energies. Table I summarises the collected number of events as well as the corresponding integrated luminosity.

TABLE I. Collision systems, centre-of-mass energies and corresponding number of events and integrated luminosities of data sets used in the presented measurements of charm baryon production.

	$\sqrt{s}$ [TeV]	N_ev	$\mathcal{L}_\mathrm{int}$	baryons
pp	5.02	10^9	$19.5\,\mathrm{nb}^{-1}$	Λ_c^+, Ξ_c^0
pp	13	$1.9 \cdot 10^9$	$32\,\mathrm{nb}^{-1}$	Λ_c^+, $\Sigma_c^{0,++}$ $\Xi_c^{0,+}$, Ω_c^0
p–Pb	5.02	$6 \cdot 10^8$	$287\,\mu\mathrm{b}^{-1}$	Λ_c^+

TABLE II. Charm baryons measured in the analyses presented in this article.

	$m_{\rm inv}$ $[\mathrm{GeV}/c^2]$	$c\tau$ $[\mu\mathrm{m}]$	decay (BR [%])
Λ_c^+	≈ 2.286	≈ 60	$\mathrm{pK}^-\pi^+$ (6.28) $\mathrm{pK^0_S} \to \mathrm{p}\pi^+\pi^-$ (1.1)
$\Sigma_c^{0,++}$	≈ 2.454	-	$\Lambda_c^+\pi^{-,+}$ (≈ 100) (7.39, above Λ_c^+ decay channels)
Ξ_c^0	≈ 2.468	≈ 46	$\Xi^- e^+\nu_e$ (1.8), $\Xi^-\pi^+$ (1.43)
Ξ_c^+	≈ 2.470	≈ 136	$\Xi^- 2\pi^+$ (2.86)
Ω_c^0	≈ 2.695	≈ 80	$\Omega^-\pi^+$ (0.51) (from theoretical calculations)

3. Charm production and hadronisation

Table II lists all charm baryons of interest in the presented analyses along with their invariant mass, decay length, and branching ratios of the studied decay channels. All values were taken as reported by the Particle Data Group [13] except for the $\Omega_c^0 \to \Omega^-\pi^+$ branching ratio which has been calculated in Ref. [14].

3.1. Λ_c^+ production

Λ_c^+ production was measured in pp collisions at a centre-of-mass energy of $\sqrt{s} = 13\,\mathrm{TeV}$ as a function of primary-particle multiplicity [15]. The bottom row of Fig. 1 shows the baryon-to-meson production ratio Λ_c^+/D^0 as a function of transverse momentum p_T.

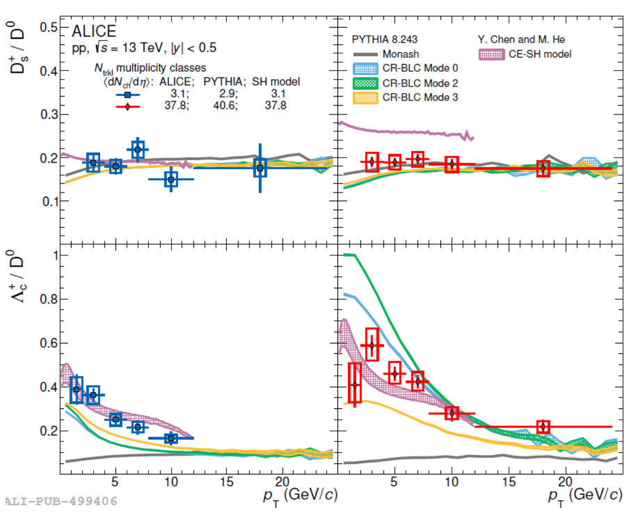

FIGURE 1. Meson-to-meson ratio $\mathrm{D_s^+/D^0}$ *(top row)* and baryon-to-meson ratio Λ_c^+/D^0 *(bottom row)* in the lowest *(left column)* and highest *(right column)* multiplicity interval and as a function of transverse momentum. Experimental results are compared to different theory predictions (see text for discussion).

It is clearly underestimated by the prediction of Pythia8 [16] with Monash tune [17] which is approximately flat at ≈ 0.1. In that case, hadronisation is tuned to results obtained in ^{e} and electron–proton (e^-p) collisions and its description is based on standard string fragmentation. On the other hand, models including colour reconnection beyond leading colour (CR-BLC) [18] are able to describe the shape as well as the observed trend with multiplicity of the experimental data although they tend to overestimate the data at lower p_T. A good agreement with the measured Λ_c^+/D^0 yield ratios is observed with the Canonical-Ensemble Statistical Hadronisation (CE-SH) model [19], which is based on a statistical hadronisation model, including augmented excited charm baryon states according to the relativistic quark model (RQM) [20], and it can also better describe the low p_T region.

On the contrary, the meson-to-meson ratio $\mathrm{D_s^+/D^0}$, shown in the top row of Fig. 2, is flat within uncertainties and well described by the theoretical prediction, even if overestimated at high multiplicities by the CE-SH model. Both results together point to modified hadronisation mechanisms beyond pure in-vacuum fragmentation in the case of charm hadron production. In addition, the Λ_c^+/D^0 ratio develops a shape that becomes steeper with increasing multiplicity, which hints at an increasing modification of the p_T spectra with multiplicity. As observed with the recent measurement from ALICE of the Λ_c^+/D^0 ratio in pp and p–Pb collisions at $\sqrt{s_\mathrm{NN}} = 5.02\,\mathrm{TeV}$ [8], the Λ_c^+/D^0 at low-intermediate p_T are higher than measurements performed with ^{e} collisions, also in the lowest multiplicity classes.

3.2. $\Sigma_c^{0,++}$ production

The first measurement of $\Sigma_c^{0,++}$production in hadronic collisions was achieved by the ALICE collaboration in pp colli-

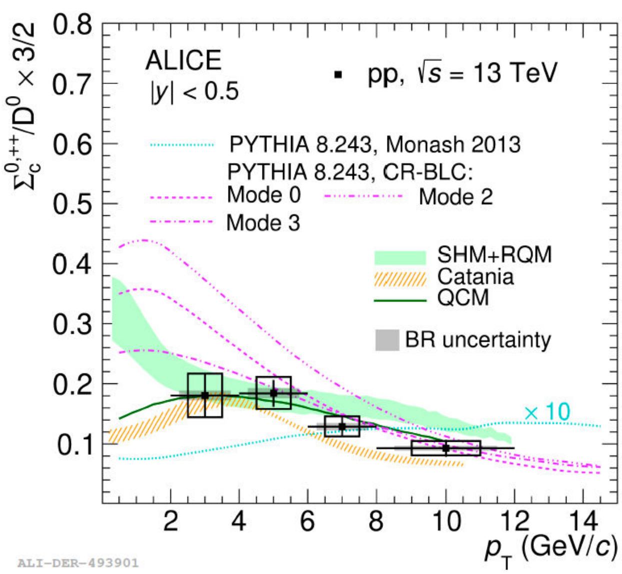

FIGURE 2. Baryon-to-meson ratio $\Sigma_c^{0,++}/\mathrm{D}^0$ as a function of transverse momentum. Experimental results are compared to different theory predictions (see text for discussion).

sions at $\sqrt{s} = 13\,\text{TeV}$ [10]. The ratio with respect to the D^0 was computed as shown in Fig. 2.

The ratio was scaled by the factor 1.5 to account for the Σ_c^+ baryon. Also in this case the experimental results show a slight slope, however less pronounced compared to the Λ_c^+/D^0 ratio. Pythia8 [16] with Monash tune [17] underestimates the data and does not describe the shape. Similarly to the Λ_c^+/D^0 ratio, the CR-BLC tunes [18] overestimate the ratio at low p_T but different to the Monash tune they exhibit a shape which successfully describes the intermediate and high p_T data points. The SH model [19] augmented with additional excited charm baryon states according to RQM [20] describes the shape and order of magnitude. Also the Catania model [21], which includes partonic coalescence in addition to in-vacuum fragmentation, is able to describe the data well within uncertainties. Another quark (re-)combination mechanism (QCM) model [22] also describes the data well within uncertainties. In this case charm quarks can combine with equal-velocity light quarks to form hadrons.

As an additional result of this analysis, a substantial feed-down fraction of Λ_c^+ of ≈ 0.4 was measured [10] which however is not sufficient to explain the increased Λ_c^+/D^0 ratio discussed in Sec. 3.1.

3.3. Ξ_c^0 and Ξ_c^+ production

Ξ_c^0 and Ξ_c^+ production was measured in pp collisions at $\sqrt{s} = 13\,\text{TeV}$ by the ALICE Collaboration [23]. Concerning the ratio of the branching fractions $\mathrm{BR}(\Xi_c^0 \to \Xi^- e^+ \nu_e)$ / $\mathrm{BR}(\Xi_c^0 \to \Xi^- \pi^+)$, a decrease of the overall uncertainty by a factor 3 was achieved compared to the current value reported by the Particle Data Group [13]. As seen in Fig. 3, among all

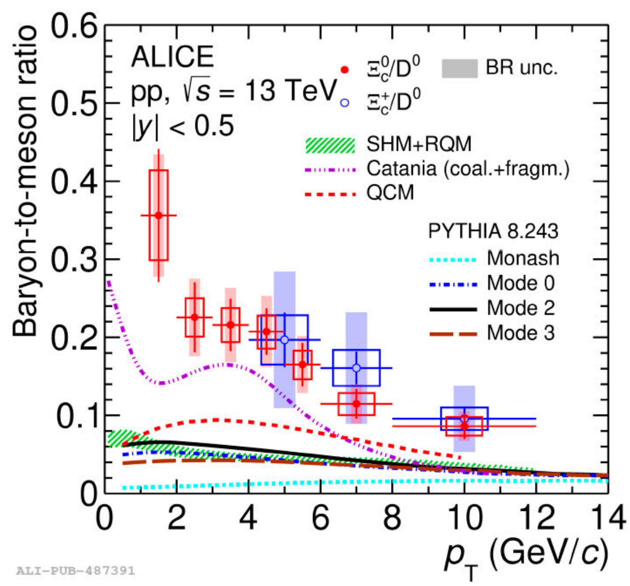

FIGURE 3. Baryon-to-meson ratios Ξ_c^0/D^0 (red) and Ξ_c^+/D^0 (blue) as a function of transverse momentum. Experimental results are compared to different theory predictions (see text for discussion).

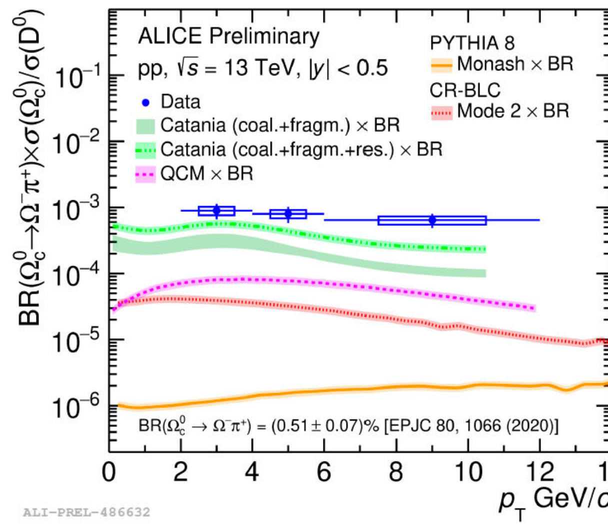

FIGURE 4. Baryon-to-meson ratio Ω_c^0/D^0 as a function of transverse momentum. Experimental results are compared to different theory predictions (see text for discussion).

compared predictions the Catania model [21] is closer to the data while the others underestimate them.

This is supported by another measurement of Ξ_c^0 production in pp collisions at $\sqrt{s} = 5.02\,\text{TeV}$ by ALICE [23].

3.4. Ω_c^0 production

As a preliminary result, the production of the Ω_c^0 baryon was measured for the first time in hadronic collisions by ALICE. Its branching ratio $\mathrm{BR}(\Omega_c^0 \to \Omega^- \pi^+)$ was provided by theoretical calculations [14]. As in the case of the $\Xi_c^{0,+}/\mathrm{D}^0$ ratio, the Catania model [21] is closest to the experimental data while other predictions underestimate the data as shown in Fig. 4. Another observation is the approximately flat shape of the ratio compared to the ratios discussed before. In this analysis, also the baryon-to-baryon production ratio with respect to the Λ_c^+ was computed and again all predictions but the one from the Catania model [21] significantly underestimate the data.

4. Charm cross section and fragmentation fractions

The charm production cross section per unit of rapidity in the fiducial rapidity window of $|y| < 0.5$ was measured in pp collisions at $\sqrt{s} = 5.02\,\text{TeV}$ [12], for the first time accounting for charm baryon production measurements of Λ_c^+ and Ξ_c^0. Its value is found to be $(\mathrm{d}\sigma^{c\bar{c}}/\mathrm{d}y)|_{|y|<0.5} = 1165 \pm 44(\text{stat})^{+134}_{-101}(\text{syst})\,\mu\text{b}$. Here, the Ξ_c^+ was accounted for by scaling the contribution of Ξ_c^0 by a factor of 2 and asymmetric errors were derived to account for a potentially sizeable contribution of Ω_c^0. In addition, the previously measured values obtained at $\sqrt{s} = 2.76\,\text{TeV}$ and $\sqrt{s} = 7\,\text{TeV}$ were updated accounting for the latest measurements of baryon-to-meson ratios presented above. This results in an increase

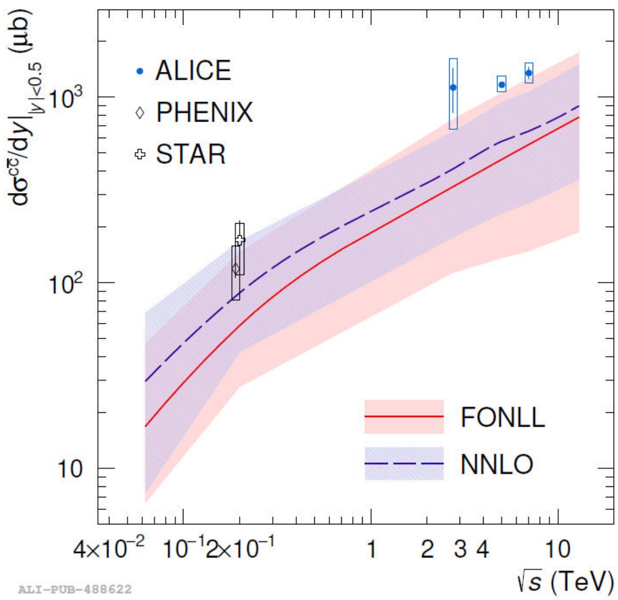

FIGURE 5. Charm production cross section as a function of centre-of-mass energy compared to FONLL and NNLO calculations.

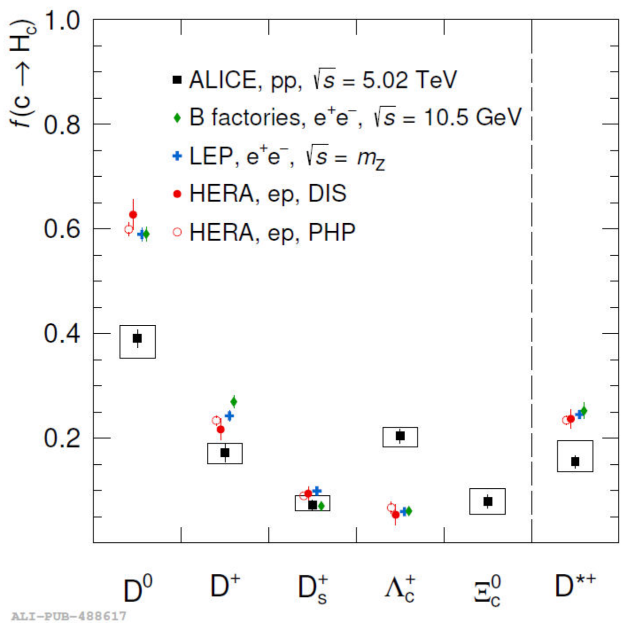

FIGURE 6. Fragmentation fractions measured in pp collisions at $\sqrt{s} = 5.02$ TeV compared to previous measurements in smaller collision system such as ^{e} and e^-p.

of about 40% compared to the previous measurements. Figure 5 shows the charm cross section per unit rapidity at midrapidity as a function of the centre-of-mass energy. The data points lie on the upper edge of the theoretical FONLL and NNLO predictions but are overall in agreement within uncertainties.

Fragmentation fractions (FF) of various charm baryons and mesons are presented in Fig. 6 in comparison with other results from smaller collision systems such as ^{e} and e^-p. The ALICE data points were obtained from pp collisions at $\sqrt{s} = 5.02$ TeV in the rapidity window of $|y| < 0.5$ [12]. Due to the most recent Λ_c^+/D^0 measurements, the current extracted value of the Λ_c^+ FF lies significantly higher compared to previous measurements while the D^0 FF is lower. The Ξ_c^0, which has been accounted for the first time, is seen to indeed have a sizeable contribution to the total charm cross section. Note that the D^{*+} feeds into the $D^0$and D^+contributions via its decays.

5. Conclusion

Various production measurements of charm baryons were presented. In particular the $\Sigma_c^{0,++}$ and the Ω_c^0 productions were measured in hadronic collisions for the first time. The most recent measurement of the total charm cross section also incorporates results from charm baryon measurements of Λ_c^+ and Ξ_c^0 and it was shown that the FF of the Ξ_c^0 introduces a sizeable contribution. Accounting for the latest results of the Λ_c^+/D^0 ratio, the most recent values of the $\Lambda_c^+(D^0)$ turned out to be significantly higher(lower) compared to results obtained in smaller collision systems.

The various results from different baryon-to-meson ratios differ from predictions where the hadronisation has been tuned to measurements obtained in ^{e} collisions. Models, which were originally developed to describe hadronisation in heavy-ion collisions, on the other hand show an overall better agreement with the data. The presented results hint at modifications of the hadronisation mechanisms beyond pure in-vacuum fragmentation even in pp collisions.

1. B. Andersson *et al.*, Parton fragmentation and string dynamics, *Phys. Rep.* **97** (1983) 231, https://doi.org/10.1016/0370-1573(83)90080-7.

2. J. C. Collins *et al*., Factorization of Hard Processes in QCD, Adv. Ser. Direct. *High Energy Phys.* **5** (1989) 1, https://doi.org/10.1142/9789814503266_0001.

3. B. A. Kniehl *et al*., Collinear Subtractions in Hadroproduction of Heavy Quarks, *Eur. Phys. J. C* **41** (2005) 199, https://doi.org/10.1140/epjc/s2005-02200-7.

4. B. A. Kniehl *et al*., Inclusive Charmed-Meson Production at the CERN LHC, *Eur. Phys. J. C* **72** (2012) 2082, https://doi.org/10.1140/epjc/s10052-012-2082-2

5. M. Cacciari *et al*., The p_T Spectrum in Heavy-Flavour Hadroproduction, *JHEP* **05** (1998) 007, https://doi.

org/10.1088/1126-6708/1998/05/007.

6. M. Cacciari *et al.*, Theoretical predictions for charm and bottom production at the LHC, *JHEP* **10** (2012) 137, https://doi.org/10.1007/JHEP10(2012)137.
7. ALICE Collaboration, Λ_c^+ production in pp collisions at $\sqrt{s} = 7\,\mathrm{TeV}$ and in p–Pb collisions at $\sqrt{s_{NN}} = 5.02\,\mathrm{TeV}$, *JHEP* **04** (2018) 108, https://doi.org/10.1007/JHEP04(2018)108.
8. ALICE Collaboration, Λ_c^+production in pp and p–Pb collisions at $\sqrt{s_{NN}} = 5.02\,\mathrm{TeV}$, *Phys. Rev. C* **104** (2021) 5, https://doi.org/10.1103/PhysRevC.104.054905.
9. CMS Collaboration, Production of Λ_c^+ baryons in proton–proton and lead–lead collisions at $\sqrt{s_{NN}} = 5.02\,\mathrm{TeV}$, *Phys. Lett. B* **803** (2020) 135328, https://doi.org/10.1016/j.physletb.2020.135328.
10. ALICE Collaboration, Measurement of prompt D^0, Λ_c^+, and $\Sigma_c^{0,++}$(2455) production in ppcollisions at $\sqrt{s} = 13\,\mathrm{TeV}$, e-Print arxiv:2106.08278 (2021).
11. ALICE Collaboration, The ALICE experiment at the CERN LHC, *JINST* **3** (2008) S08002, https://doi.org/10.1088/1748-0221/3/08/s08002.
12. ALICE Collaboration, Charm-quark fragmentation fractions and production cross section at midrapidity in pp collisions at the LHC, e-Print arxiv:2105.06335 (2021).
13. P. A. Zyla *et al*. (Particle Data Group), Review of Particle Physics, *Prog. Theor. Exp. Phys.* **2020** (2020) and 2021 update, 083C01.
14. Y. Hsiao *et al.*, Charmed Ω_c weak decays into Ω in the light-front quark model, *Eur. Phys. J. C* **80** (2020) 1066, https://doi.org/10.1140/epjc/s10052-020-08619-y.
15. ALICE Collaboration, Observation of a multiplicity dependence in the p_T-differential charm baryon-to-meson ratios in proton–proton collisions at $\sqrt{s} = 13\,\mathrm{TeV}$, e-Print arxiv:2111.11948 (2021).
16. T. Sjostrand *et al.*, A Brief Introduction to PYTHIA 8.1, *Comput. Phys.* Commun. **178** (2008) 852, https://doi.org/10.1016/j.cpc.2008.01.036.
17. P. Skands *et al.*, Tuning PYTHIA 8.1: the Monash 2013 Tune, *Eur. Phys. J. C* **74** (2014) 8, https://doi.org/10.1140/epjc/s10052-014-3024-y.
18. R. Jesper *et al.*, String Formation Beyond Leading Colour, *JHEP* **08** (2015) 003, https://doi.org/10.1007/JHEP08(2015)003.
19. Y. Chen, M. He, Charged-particle multiplicity dependence of charm-baryon-to-meson ratio in high-energy proton-proton collisions, *Phys. Lett. B* **815** (2021) 136, https://doi.org/10.1016/j.physletb.2021.136144.
20. D. Ebert *et al*., Spectroscopy and Regge trajectories of heavy baryons in the relativistic quark-diquark picture, *Phys. Rev. D* **84** (2011) 014, https://doi.org/10.1103/PhysRevD.84.014025.
21. V. Minissale, *et al*., Charm Hadrons in pp collisions at LHC energy within a Coalescence plus Fragmentation approach, *Phys. Lett. B* **821** (2021) 136, https://doi.org/10.1016/j.physletb.2021.136622.
22. V. Minissale, *et al.*, New feature of low p_T charm quark hadronization in pp collisions at $\sqrt{s} = 7\,\mathrm{TeV}$, *Eur. Phys. J. C* **78** (2018) 344, https://doi.org/10.1140/epjc/s10052-018-5817-x.
23. ALICE Collaboration, Measurement of the cross sections of Ξ_c^0 and Ξ_c^+ baryons and branching-fraction ratio BR($\Xi_c^0 \to \Xi^- e^+ \nu_e$)/BR($\Xi_c^0 \to \Xi^- \pi^+$) in pp collisions at 13 TeV, e-Print arxiv:2105.05187 (2021).
24. ALICE Collaboration, Measurement of the production cross section of prompt Ξ_c^0 baryons at midrapidity in pp collisions at $\sqrt{s} = 5.02\,\mathrm{TeV}$, e-Print arxiv:2105.05616 (2021), https://doi.org/10.1007/JHEP10(2021)159.